Received: 25 August 2023 | Revised: 12 October 2023 | Accepted: 13 October 2023 | Published online: 23 October 2023

RESEARCH ARTICLE

Journal of Optics and Photonics Research
2024, Vol. 1(1) 32–42
DOI: 10.47852/bonviewJOPR32021587

BON VIEW PUBLISHING

# Role of Micro-Architectures on Insects' Elytra Affects the Nanomechanical and Optical Properties: Inspired for Designing the Lightweight Materials

**Jeevan Jyoti[1],* and Sangita Tripathy[2]**

[1]*School of Mechanical Engineering Department, Indian Institute of Technology Ropar, India*

[2]*Council of Scientific and Industrial Research, National Physical Laboratory, India*

**Abstract:** The structural coloration of insects has received significant attention in the field of nanophotonic, which has related properties with biophotonic crystals. The main focus of this study is on structural and mechanical features of wasp and beetle elytra such as Chrysidinae (the specimen of parasitoid or kleptoparasitic wasp), *Rhomborhina gigantea* (RG is the specimen of bettle in the family of Cetoniidae), and *Chrysolina coerulans* (CC is a species of beetle in the family Chrysomelidae). The nanostructures present on the surface of elytra show the optical and deformable material properties. Surface morphology has been measured by scanning electron microscopy and atomic force microscopy (AFM). The depths of the hemispherical cavities present on the elytra have been analyzed using AFM. The optical and nanomechanical properties of the beetle elytra have also been studied. To measure the reflectivity in transverse electric and TM mode, UV-visible spectroscopy has been used. The value of the average index of refraction $n_{av}$ is observed as 1.8 in all three species and the half-pitch of elytra's varies from 0.139–0.136 μm in CC, 0.123–0.114 μm in Chrysidinae, and 0.154–0.161 μm in RG. Nanoindentation was used to measure the modulus and hardness of the different beetle's elytra. Higher value of elastic modulus (1.72 GPa) and hardness (0.89 GPa) in RG of elytra plays a significant role in resisting force. The photonic structure exhibits optical intrinsic color mixing properties, which are used in the anticounterfeiting fields (currency and passport identification codes). The structural properties of beetle elytra would help to design the lightweight, high strength, anti-coating sensor, color-changing micro air vehicles, and novel optical materials.

**Keywords:** elytra, reflectivity, nanomechanical, hemispherical cavities

## 1. Introduction

Over the 400 millions of years, natural creatures (insects) have created a significant interest of researchers in their biological uniqueness of structures and optical properties. Numbers of studies have reported inventions on the biophysics of natural creatures. Insects are considered to be an outstanding example of the photonic research subjects due to their diversity, coloration, and abundance (Berthier, 2007; Grier, 2003; Parker, 2000; Sharma et al., 2009; Wu et al., 2023). The disordered structure of the natural creature's wing surface inspired the photonic community to design structure with multifunctional properties. Researchers have generated significant interest on the insect due to their bright and varied colors owing to their texture or ornaments. The morphology and structure of their biological systems have made these insects of genius creation of nature (Lam et al., 2023; Lee et al., 2021; Zhou et al., 2019). Insects exhibit a variety of photonic nanostructures, which in turn form their structural colors. The photonic properties of the insects are seen through the different geometric structure and morphology of the elytra, which depends on the transportation of light through the periodic photonic nanostructures of the elytra (Zhao et al., 2012). The photonic study (biophotonic) of these natural creatures reveals the elegant and diverse examples regarding the wavelength and structural features that produces variety of experimental colors through the thin layered or multilayered interference, light scattering, diffraction, and often with the contribution of pigmentation as well (Mouchet et al., 2023; Sharma et al., 2009). Compared with the pigment color, the structural color is much more efficient in energy consumption and in the use of light (Ospina-Rozo et al., 2023).

The coloration exhibited by insects is attributed to selective scattering wavelength of light by microscopic features. When the incident light interacts with the nanostructure of biological insects, it leads to scattering of light in all directions (Srinivasarao, 1999; Vigneron et al., 2007). The color-producing angle can possess a strong directionality and color is only seen at a certain angle. The most common study in this context is the wing of the morpho butterfly family (Kinoshita, 2008). The interaction of light with the wing of the butterfly provides a fabulously blue color showing the angle-dependent characteristic (Dehmel et al., 2017; England et al., 2017; Fu et al., 2017; Kertész et al., 2021; Lloyd & Nadeau, 2021; Starkey & Vukusic, 2013). The angle-dependent coloration

*Corresponding author: Jeevan Jyoti, School of Mechanical Engineering Department, Indian Institute of Technology Ropar, India. Email: jeevanjyoti.npl@gmail.com

properties are caused by the periodic variations in the refractive index created by complicated structure on the bodies of the insects.

Scientists are continuously concentrating on the development of new photonic technology inspired from nature. The number of research studies suggests that nature has developed many technologies that can solve everyday problems (Gan et al., 2016; Karthaus, 2012; Zhang et al., 2019). The biomimetic techniques have been widely used in recent years for designing the lightweight and high strength materials in the field of military, aerospace, aircraft, construction, automotive, and so on (Koch et al., 2009; Reddi et al., 2012; Zhou et al., 2020). Researchers are putting the efforts on designing the materials, which are mimic elytra of the insects. The forewing of the beetle plays an essential role in protecting the body and contributes to the flight. Beetles develop their forewing into elytra, which are predominantly composed of chitin fibers, collagen, amylase, etc., which produce a rigid texture (Chen et al., 2002; Chen et al., 2022). The excellent mechanical properties of the elytra, such as high density, toughness, anisotropy, and the ability of self-healing, are very inspiring properties (Guo et al., 2014). Several previous elytra-based studies have focused on the structural coloration (Liu et al., 2008), microstructure and the arrangement of chitin fiber (Gorb et al., 2002; Heepe et al., 2016; Li et al., 2017), mechanical properties of the elytra (Guo et al., 2012; Yu et al., 2013; Li et al., 2017), mechanism of coupling between the elytra (Gorb & Goodwyn, 2003; Frantsevich et al., 2005; Zhou et al., 2015), and elytra surface inspired structural design, manufacturing, and study of mechanical properties exhibited by these insect (Chen & Wu, 2013; Guo et al., 2012; Sun et al., 2019). Several research groups have studied the polarization properties of beetle elytra due to their bright and shiny colors. Exoskeleton (forewing), i.e., the upper surface of beetle elytra, represents iridescence arising from the physical nature of their photonic structure. The optical reflectors are present on the surface of the exocuticle layer of the beetle, which are responsible for structural colorations and insects (Brink et al., 2007; Neville & Caveney, 1969). The upper surface of the exocuticle of the beetle elytra consists of the periodically spaced layered structure in which each layer consists of enormous amounts of microfibrils. Each layer of the beetle elytra acts as an optically anisotropic medium having a larger index for reflection of the polarized lights along the fibers than that of perpendicular polarized light (Brink et al., 2007). Michelson (1911) reported the optical properties of the exocuticle elytra and their ability to reflect (mainly) at left circularly polarized light and not at right circularly polarization light.

Herein, the main purpose of this research work is to study the photonic materials present on the beetle elytra with variable structural colors that keep on changing, which depends upon the reflectivity. We examined their morphology by optical microscope, scanning electron microscopy (SEM), and atomic force microscopy (AFM). The structural, optical, and nanomechanical properties of the wasp and beetle elytra were analyzed along with the mechanism behind the mechanical behavior. Additionally, we measured the biomechanical properties of the beetle elytra such as elastic modulus, hardness, and stiffness. These properties of tunable structural color materials are desirable in many novel optical technologies.

## 2. Materials and Methods

### 2.1. Specimens

In this work, the elytra of wasp and beetles such as Chrysidinae (wasp), *Rhomborhina gigantea* (RG), and *Chrysolina coerulans* (CC) (beetles) were caught the near to Indian Institute of Technology Ropar, India because of their similarity in dimensions to that of the elytra. All the wasp and beetle elytra included in this study were adults and 18 samples were used in our analysis. The specimens were cut down with the help of a surgical blade near the highest point of the elytra for microstructure and nanoindentation analysis.

### 2.2. Scanning electron microscopy

The JEOL SEM was used to determine the morphology of the exoskeleton surface of the elytra. The sample preparation process for SEM analysis was followed as: firstly, the elytra were peeled off from the body. After that, the elytra were washed with ethanol and followed by ultrasonic cleaner for 10 min to remove the dust and impurities and thereafter dried in the oven at 40°C for 12 h. The elytra samples were coated with the palladium metal using the sputtering and surface analysis of the wing at 20 kV was carried out.

### 2.3. Structural analysis (optical micrographs)

The structural investigation of the elytra was analyzed using the reflective light stereo optical microscopic (Leica S8 APO) with Leica EC3 camera and software installed on a desktop. The optical images of the three different elytra were used to get detailed structural information of elytra.

### 2.4. Atomic force microscopy

The microstructure analysis of the exoskeleton elytra was investigated by multimode of AFM (BrukerMultimode 8, Bruker, Germany) in area 20 × 20 μm of the Chrysidinae and other two elytra by reducing the size to 10 × 10 μm. Roughness analysis (valleys), size of nanostructures, the height of hemispherical cavities, and other analyses were carried out using nanoscale analysis software (tapping mode). These studies were carried out in tapping mode under air-ambient conditions (temperature of 20–30°C and 60–75% RH).

### 2.5. Optical method (UV-Vis-NIR spectrophotometer)

Angle-dependent reflectivity was measured by the UV-Vis-NIR spectrophotometer (Perkin Elmer Lambda 950 UV/Vis/NIR spectrophotometer, USA) in reflection mode. The exoskeleton of elytra samples was properly mounted in the sample holder. The reflected light was collected using the photomultiplier tube. The estimated diameter of the spot size of the reflected light was observed to be 5 mm. The polarizer was mounted in the path of incident beam in transverse electric (TE) and transverse magnetic (TM) polarization mode of light with wavelength range 450–700 nm.

Optical reflection can be obtained when the Bragg's condition is satisfied (Neville & Caveney, 1969):

$$\lambda = n_{av} P_0 \cos\varnothing_1 = 2 n_{av} P_H \cos\varnothing_1 \quad (1)$$

where λ is the vacuum wavelength of the reflection peak, angle of the propagation of the medium is $\varnothing_1$ and $n_{av}$ is the average refractive index, $P_0$ the full pitch of the microfibrils is of 360° rotation. The structure looks and behaves same after the 180° rotation, the value of half-pitch is given by $P_{H=} \frac{P0}{2}$. According to Snell's law angle, $\varnothing_1$ is related to the incidence of angle $\varnothing_0$ in the air (Brink et al., 2007).

$n_0 \sin\varnothing_0 = n_{av} \sin\varnothing_1$, which changes equation (1) to

$$\sin^2\varnothing_0 = -\frac{1}{P_0^2}\lambda^2 + n_{av}^2 \quad (2)$$

Plotting the fitting equation a $\sin^2\varnothing_0$ versus $\lambda^2$, the independent values for the pitch and average refractive index of the structure of the elytra of beetle are analyzed.

## 2.6. Nanoindentation

The nanoindentation tests on the exoskeleton surface of the forewing of three different elytra samples were carried out experimentally. The samples of elytra were cut with the help of diamond cutter, mounted in the epoxy resin and polished. The nanoindentation test has been performed using TI 950 Tribo-Indenter (Hysitron, Inc., Minneapolis, MN, USA) with a Berkovich diamond tip with the nominal radius of curvature 100 nm. The loading process includes maintaining a constant displacement of 1000 nm and to measure the response of force. The important parameters like maximum load ($P_{max}$), maximum displacement ($h_{max}$), stiffness $S = \frac{dP}{dh}$, and penetration depth ($h_f$) were calculated using load ($P$) versus penetration depth curve ($h$).

The value of hardness is calculated from (Oliver & Pharr, 2004)

$$H = \frac{P_{max}}{A} \quad (3)$$

where the symbol $A$ is the contact area at $P_{max}$. The elastic modulus ($E_r$) is related to the stiffness as:

$$S = 2\beta\sqrt{\frac{A}{\pi}}E_r \quad (4)$$

where $\beta$ is a constant depending on the geometry of the indenter.

## 3. Result and Discussion

## 3.1. Morphological studies

The exoskeleton of the elytra is observed under optical microscope, and the upper surface of the elytra is decorated with medley of points and colors, which consists of regular space lattice features that are different from other beetle exoskeletons. For the past decades, the exoskeletons (elytra) of the insects are commonly visible as they possess brilliant and shiny reflection mirror-like structure, which is attracting the eyes of people. The structural coloration of the elytra/wings is the outcome of the interactions of photonic structure and light with a featured size of wavelengths. Optical microscope is used to observe the upper surface of the elytra that showed the color pattern, due to the interference of light with the multilayered structure of beetle cuticle. Figure 1 shows the optical microscopic images of the three different elytra with same dimension in the reflection of unpolarized light, which helped in investigation of the morphology of the upper layer of the elytra structures. Using the bright-field optical microscope at the high magnification, the circular shape structures are observed on multilayered upper surface of the elytra. The exoskeleton of the elytra is observed under the microscope with the different magnification power and elytra are observed to be decorated at the borders with colors. The structure of the exoskeleton consisting of the regular space lattice features shows that each species of beetle distinguishes from each other. Figure 1(a) and (b) has bright sky-blue borders with bright blue centers and the diameters of the Chrysidinae wasp are approximately 140 μm. There are sky blue and blue areas distributed in the regions, and hemispherical cavities are detected on the surface of the exoskeleton wings. Figure 1(c) and (d) indicates the green sample of beetle (RG); the top surface is covered with the hemispherical cavities having a certain space, diameter, and height. The diameter of the RG elytra surface is approximately 68 μm. Similarly, in the case of CC beetle, the surface of the elytra beetles is covered of circular holes with the diameter approximately 63 μm as shown in Figure 1(e) and (f). The elytra of the beetle are also covered with the number of layered structures. Many researchers reported that the elytra (forewing) of the insects consist of the layered structures. The upper and lower layered structures of the insect elytra/wing are composed of the protein and chitin fiber (Iwamoto et al., 2002).

In Chrysidinae, the circular shapes like hemispherical cavities are found on the elytra surface. Using optical microscopy, beautiful shiny patterns were observed in the elytra surface. The microscopic colors are the results of light interference by multilayer structures of the wing. The pitches are too small and cannot be seen with the naked eye. The surface microstructures of these three beetles' elytra that are also observed in the SEM and AFM are discussed in the next section. AFM is a very useful technique in determining the microstructure of the elytra and wings.

AFM is an excellent instrument in the development of nanotechnology and nanoscience for the past few decades. AFM measures the deflection of the probe as it scans the surface of the samples. Many research groups have reported the surface morphology of the insect wings and elytra (Clark-Hachtel et al., 2013; Linz et al., 2016; Wang et al., 2023). Figure 2 shows the surface morphology of the elytra. AFM analysis discovered irregular-shaped nanostructures on the surface of the elytra. Figure 2(a) and (b) clearly shows the surface roughness and serrated boundaries presents on the surface exoskeleton of the elytra. The surface heights ranged from 880 to 900 nm are observed at 20 μm × 20 μm in scan. The inserted image in Figure 2(a) shows valleys in the form of peaks and troughs. The surface morphology using the AFM imaging helps in determining the depth and the width of the hemispherical cavities present on the surface. Figure 2(c), (d), (e), and (f) clearly shows the presence of hemispherical cavities with different dimensions and the wrinkles on the surface of the elytra. The depths of the exoskeleton surface of the RG are roughly lying between 270 and 600 nm. Similarly, the AFM image of CC shows the hemispherical cavities and the depth of hemispherical cavities lies between 600 and 800 nm. AFM images clearly show the texture of the exoskeleton of the elytra. It is observed that the surface of the exoskeletons is covered with many barbs over several micrometers.

The surface morphology of the elytra was investigated using the SEM. SEM is the most powerful technique, which is used to determine and analyze the surface as well as structural morphology of the wing. It helps in measuring the diameter of hemispherical cavities. The SEM images indicate the presence of setae (small hair) on the hemispherical cavities of the surface of the elytra. SEM image has illustrated that the diameters of pits are not equal. Figure 3(a) and (b) shows that the average diameter lies in the range of 70–110 μm. Similarly, trends were noticed for other two elytra. The diameters of the elytra are observed to be less than 100 μm as shown in Figure 3(c) and (d). The images of CC elytra are not seen to be perfectly circular in shape and diameter lies between 35 and 60 μm as shown in Figure 3(e) and (f). The surface morphology of the elytra made the structural analyses of the insects easy and gives some important information

**Figure 1**
**An optical micrograph of the exoskeleton of the insects (a and b) Chrysidinae, (c and d) *Rhomborhina gigantea* (RG), and (e and f) *Chrysolina coerulans* (CC) with different magnifications**

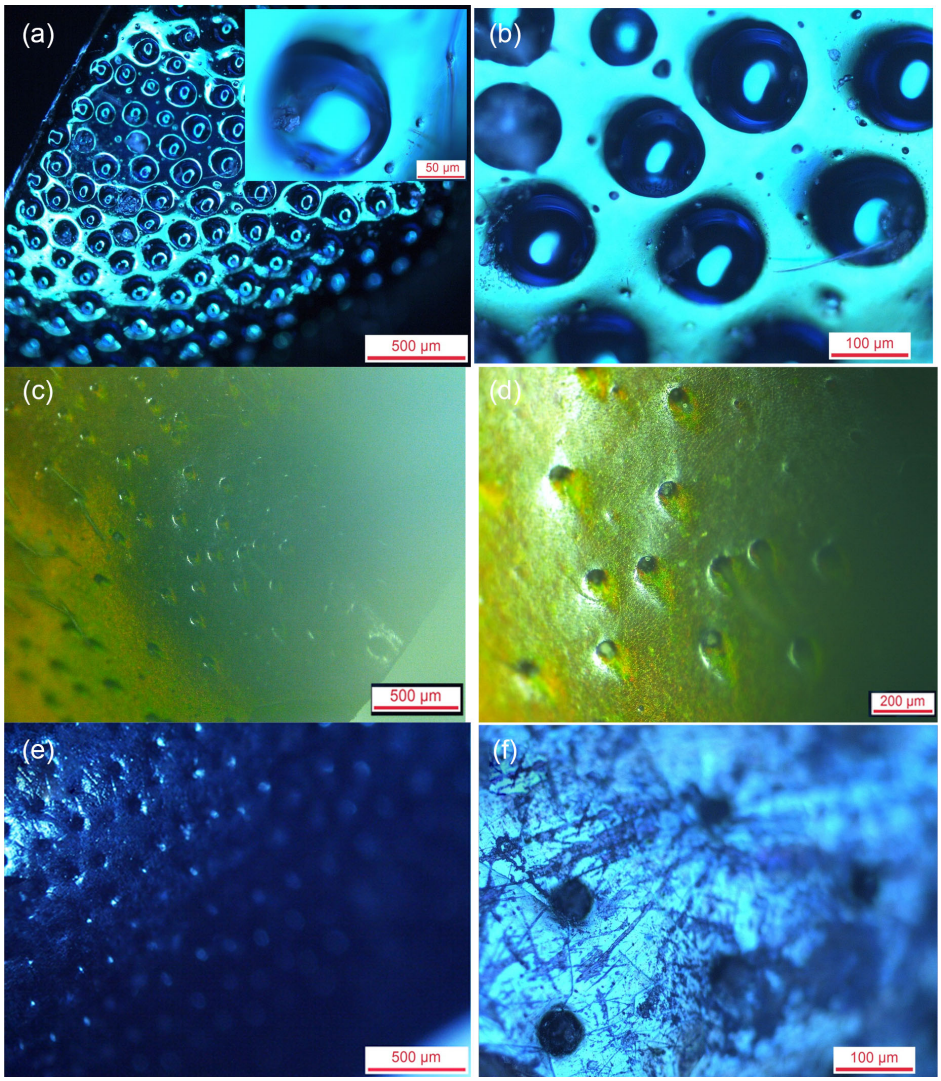


about the material development. Flying insects appear to have the contrivance for their protection and lightweight.

### 3.2. Polarization and angle-dependent reflection measurements

The angle-dependent reflection of the polarized light was studied using the UV Visible spectroscopy. The spectra for both TE and TM polarized lights were obtained using altered angular directions in the vertical plane of scattering light. Figure 4 clearly shows that the reflectance of TE and TM bands shifted hypsochromically in all three exoskeletons of elytra. The reflectance spectra strongly depend upon the angle of the incidence light. The angle of the incidence varies in the step size of 10° up to 40° following which we fixed the angle of 45° to satisfy the Fresnel law. The peak wavelength of both modes is shifted toward the shorter wavelength for all exoskeleton surfaces of the elytra as shown in Figure 4. Beyond the angle of 45°, no change in the peak shift is observed. Figure 4(a) and (b) shows the TE and TM mode of Chrysidinae exoskeleton wing. The reflection spectra of the elytron in the TE and TM polarization mode indicate that the peaks in the blue visible region experienced violet shift with increase in the incident angles (10–40°). At the higher angle of incidence, reflection peaks are independent of the incident angle. TE and TM modes of RG beetle also show the reflection peaks in yellow visible region showed a green shift with an increment in the angle of the incident (10–50°) as shown in Figure 4(c) and (d). In CC elytra beetle wing, the reflected peaks in the blue visible region shift to the violet region as the angle of incident is increased. TE and TM modes of CC beetle are shown in Figure 4(e) and (f). The layered nanostructures in elytra wings are responsible for the physical coloration of wings. The photonic structures present on the exoskeletons of the wing show the properties of multiple inner reflections due to the multilayer hemispherical cavities (grooves). At higher incident angles, the reflected peaks become independent of the incident angle and follow the Fresnel law, which shows that the colored response of exoskeletons of the beetle wing is due to ambient refractive index.

**Figure 2**
**AFM images of microstructures of three different beetle elytra surfaces (a and b) Chrysidinae, (c and d) *Rhomborhina gigantea* (RG), and (e and f) *Chrysolina coerulans* (CC) with different magnifications to calculate the heights of hemispherical voids**

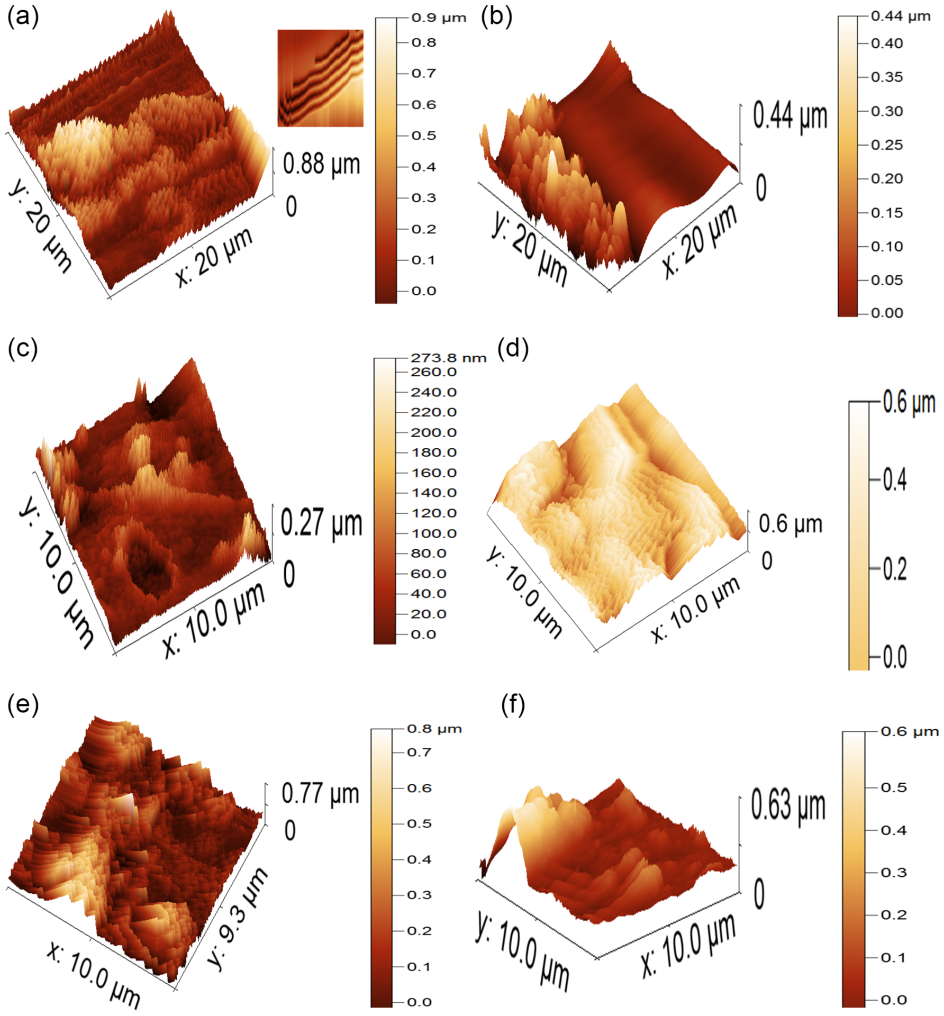


The exoskeleton of the wings composed of multiple nanostructures shows that the intensity of reflections in TE and TM polarization was neither increased nor decreased with the angle of the incident light. Figure 4 shows the opposite trend in TE and TM modes of polarization with nonexistence of single dominant reflection peak, which further designate that optical reflector existing in the wings is complex multilayer structure (Ching et al., 2014).

## 3.3. Determination of half-pitch and average refractive index

Using equation (2), we can calculate the average refractive index by extrapolating the linear fit data of Figure 5 to obtain the y-axis intercept, while the value of $-1/P_o^2$ helps to obtain the slope of linear fit for Figure 5.

For Chrysidinae beetle in TE polarization mode, the value of $n_{av} = 1.85$ and $p_h = 0.123$ µm using the linear fitting is shown in Figure 5(a). Figure 5(b) shows the TM polarization mode $n_{av} = 2.126$ and $p_h = 0.114$ µm. In the case of RG, the value of $n_{av} = 1.79$ and $p_h = 0.154$ µm in TE polarization mode is shown in Figure 5(c). For TM polarization mode, $n_{av} = 1.74$ and $p_h = 0.16$ µm (Figure 5(d)). Similarly in the case of CC, $n_{av} = 1.75$ and $p_h = 0.139$ µm in TE polarization and on the other hand $n_{av} = 1.78$ and $p_h = 0.136$ µm for TM mode of polarization calculated from Figure 5(e) and (f), respectively. The refractive index of cuticle layers of the scarabaeid beetle is experimentally found to lie between 1.5 and 1.6 (Neville & Caveney, 1969). Some researchers have found the value of 1.7 in the presence of uric acid in the cuticular reflector. The average refractive index value in the three different beetles agreed well with the reports (Scharf, 2007). The reflection of light is generally due to the difference in the Fresnel reflection coefficient between the TE and TM modes. In the single optical interface, the reflection is persuading only the TE mode because the TM mode disappears completely at the Brewster angle. The polarization capability of cavities on the exoskeleton surface of wing is defined by polarization contrast given as (Berthier et al., 2007)

$$P = \frac{R_{TE} - R_{TM}}{T_{TE} + R_{TM}} P \in [-1, 1] \quad (5)$$

where $R_{TE}$ and $R_{TM}$ are the reflectances in *TE* and *TM* modes, respectively. The value of $P = -1$ indicates that spectrum is TM and $P = +1$ for TE mode. The values of P for different elytra are given in Table 1.

**Figure 3**
**SEM images of microstructures of elytra surfaces (a and b) Chrysidinae, (c and d) *Rhomborhina gigantea* (RG), and (e and f) *Chrysolina coerulans* (CC) with different magnifications**

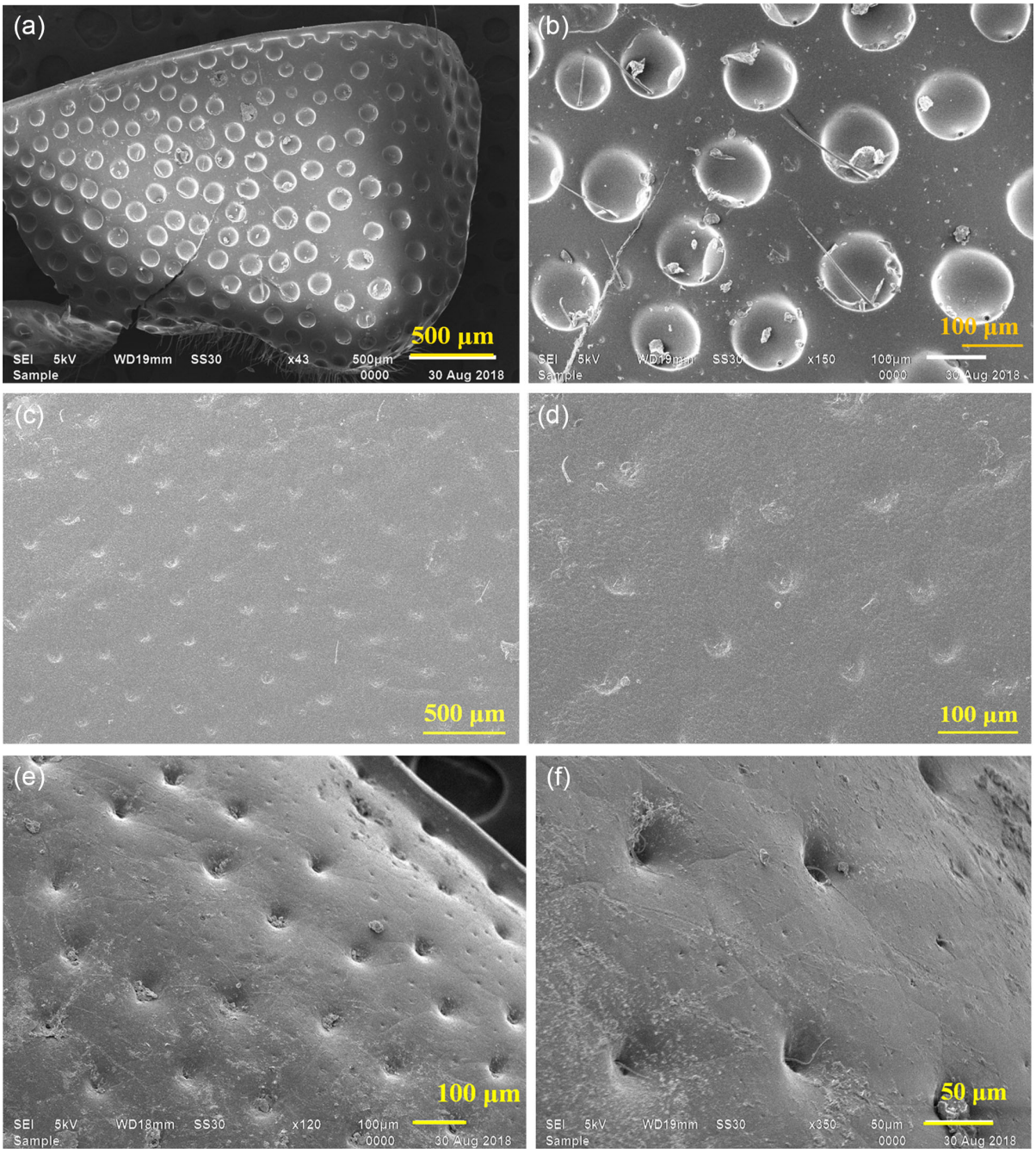


The size of the holes on the surface of the exoskeleton plays an important role in the polarization contrast. The value of polarization contrast increases from −0.026 to −0.033 in Chrysidinae, −0.0013 to 0.004 in RG, and −0.00007 to 0.0005 CC only at 10° angle reflected spectrum. It indicates that the TE mode is more reflecting than the TM mode in all three different surfaces of elytra. The polarization state of reflection may be depending on the arrangement of surface cavities. SEM image showed the presence of circular cavities on the elytra of Chrysidinae wasp. However, the AFM images clearly showed the valleys, since the light gets polarized before reaching the voids.

## 3.4. Nanomechanical

It is depicted from Figure 6(a) that the values of H for Chrysidinae, RG, and CC are 0.46, 0.89, and 0.1 GPa, respectively. A similar trend is observed in Figure 6(b) for elastic modulus property of the samples; Chrysidinae, RG, and CC values were 1.57, 1.72, and 0.23 GPa, respectively. Thus, an improvement in elastic modulus and hardness of RG beetle elytra is recorded higher than the other two beetle elytra samples. In addition to elastic modulus and hardness properties, wear resistance is also an important parameter in determining the

**Figure 4**

**Reflection spectra of three different beetle elytra (a) TE polarization of Chrysidinae, (b) TM polarization of Chrysidinae, (c) TE polarization of RG, (d) TM polarization of RG, (e) TE polarization of CC, and (f) TM polarization of CC**

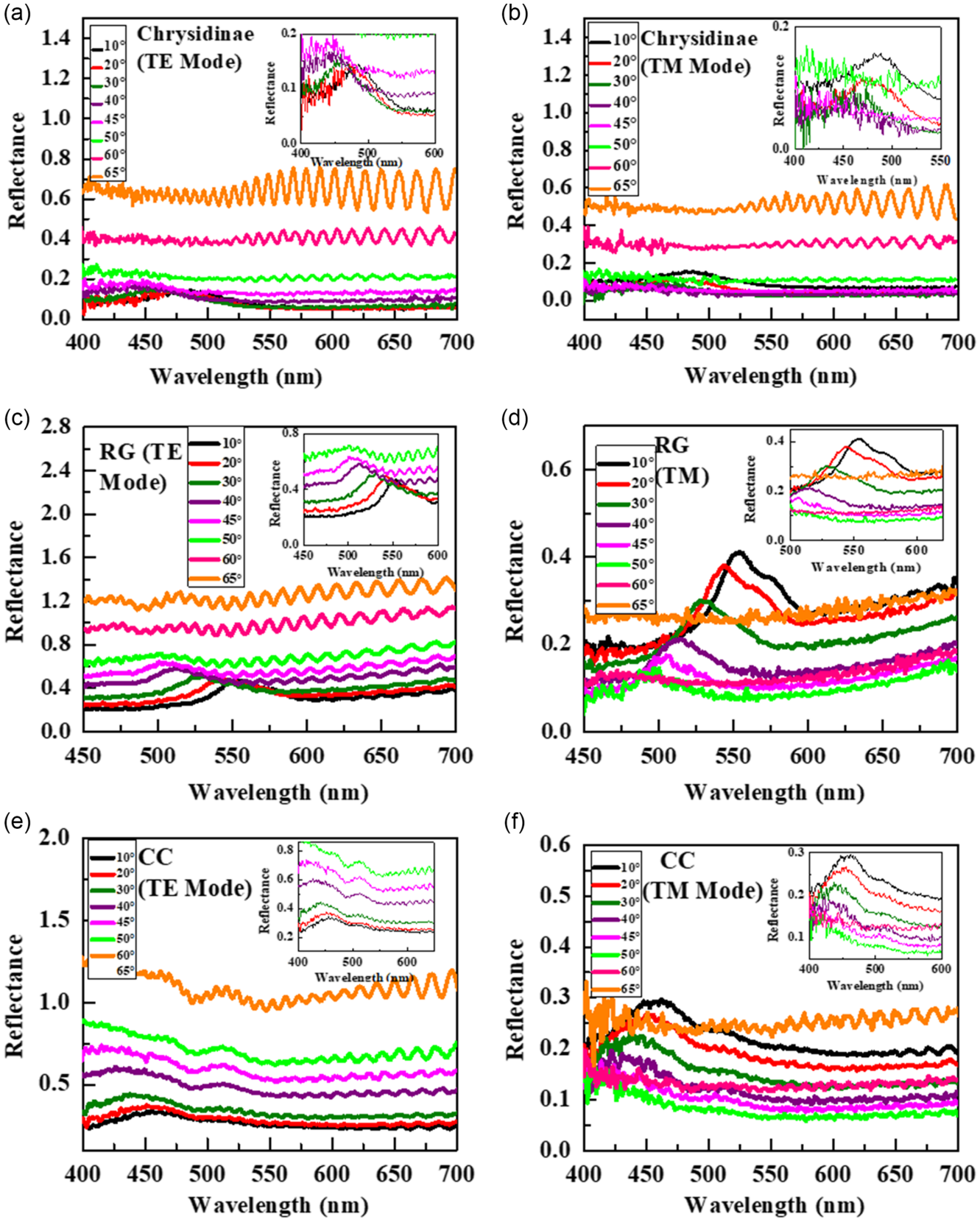

**Figure 5**
**Linear fit of peak wavelengths in (a) TE and (b) TM of Chrysidinae, (c) TE and (d) TM of RG beetle, (e) TE and (f) TM of CC beetle**

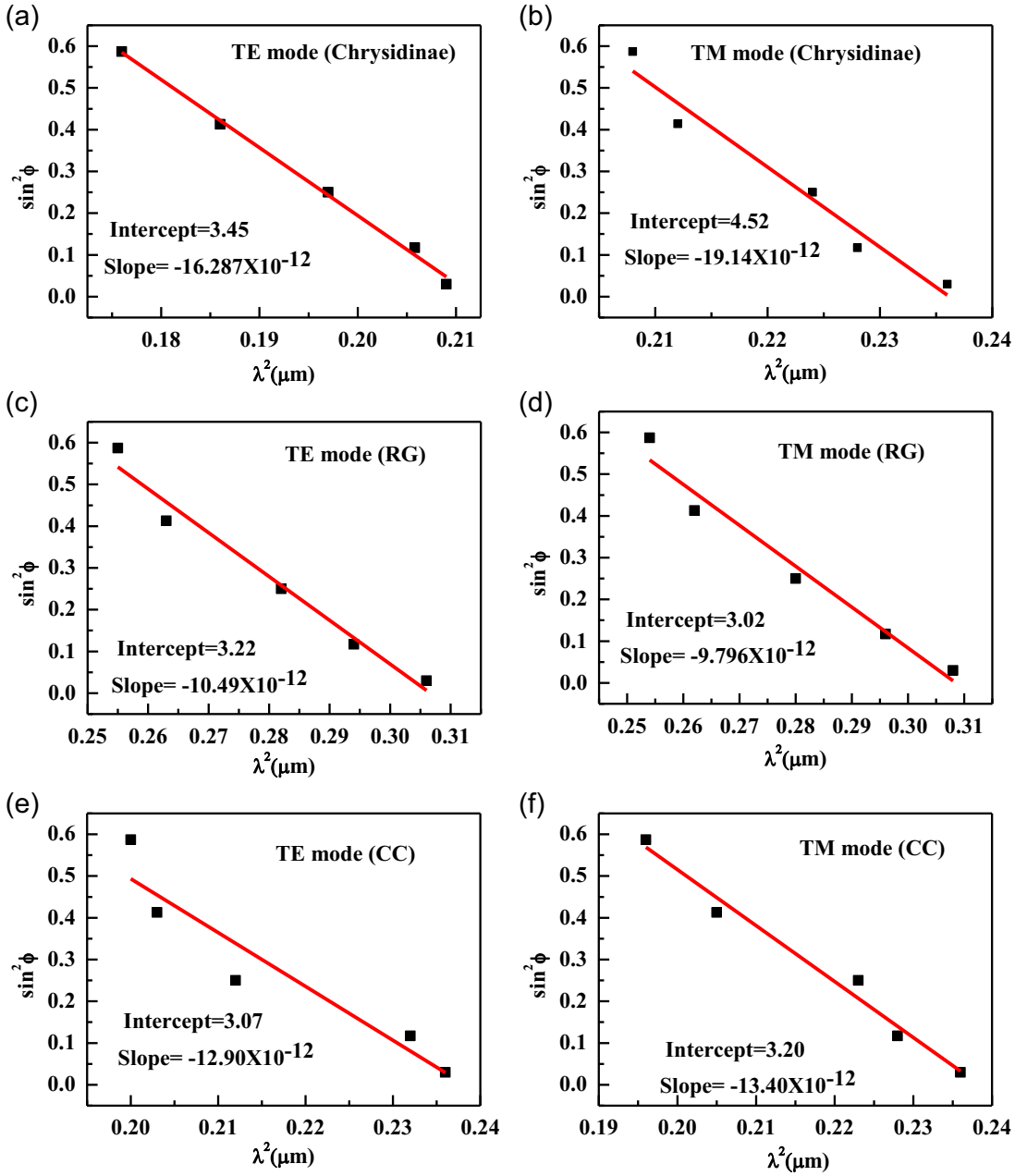


**Table 1**
**Comparison of polarization contrast P of wasp and beetles at different values using the TE and TM modes**

| Polarization contrast at different angle | Chrysidinae wasp | RG beetle | CC beetle |
|---|---|---|---|
| $P_{10}$ | −0.033 | −0.0013 | −0.00007 |
| $P_{20}$ | −0.026 | 0.002 | 0.0004 |
| $P_{30}$ | −0.032 | 0.002 | 0.0005 |
| $P_{40}$ | −0.033 | 0.004 | 0.0003 |
| $P_{45}$ | −0.032 | 0.002 | 0.00025 |
| $P_{50}$ | —— | 0.001 | 0.0005 |

behavior of elytra. The lower value of H/E in Chrysidinae signifies that the fraction of work is being consumed in plastic deformation. On the other hand, larger values of H/E for RG indicated lesser plastic deformation as shown in Figure 6(c). The estimation of contact stiffness (dP/dh)max has been verified with the elastic and plastic properties of the polymer. Stiffness is defined as the resistance of an elastic body against deformation under the load. The variations in the stiffness of beetle exoskeleton samples are shown in Figure 6(d). The value of the stiffness of Chrysidinae is 2μ N/nm and a decreasing trend was observed; behavior is seen for the other two beetle elytra samples (1.83 for RG and 0.28 for CC). The elytra of the insects are rigid, defensive against the environmental hazards, and protect the forewing.

**Figure 6**
**Variation of (a) hardness, (b) elastic modulus, (c) (H/E) indentation load, and (d) stiffness behavior of the H-E curve of different type of beetle's exoskeleton**

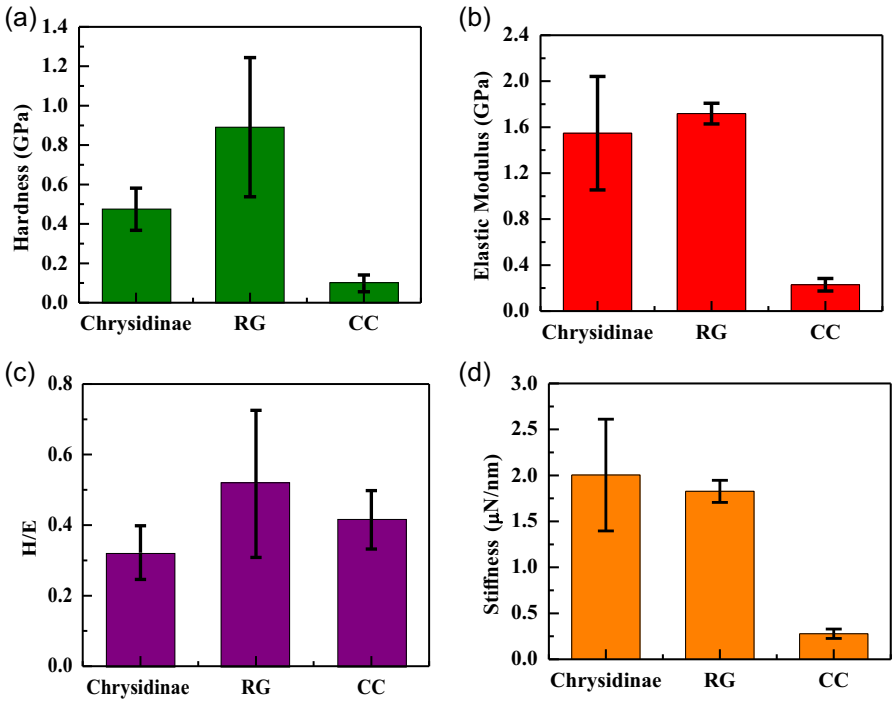


## 4. Conclusion

The conclusion of this study offers evidence to support the new level of detailed study with respect to the structural and optical properties of three different elytra of beetles. The beetle forewings are highly optimized biological structure. The forewings of beetle species involve lightweight-integrated frame structures, which consist of hemispherical cavities regions. Quantification of cavities depth, the diameter of circle, and size of the elytra were analyzed using the AFM and SEM, respectively. Optical and SEM images exposed the periodicity within the elytra of beetles. Optical and nanomechanical properties were carried out to investigate the Chrysidinae (wasp), RG and (CC (beetles) elytra. The reflectivity measurement was to support the variations in the incident angle and measured the TE and TM modes polarization. When the value of the incident angle increased, the overall intensities decreased in the TM mode and increased in the TE mode. The polarization contrast properties were also analyzed and concluded that TE mode was dominant in all three beetle samples. We also calculated the half-pitch and refractive index. In the Chrysidinae beetle, the value is $n_{av} = 1.85$ and $p_h = 0.123$ μm in the TE polarization mode. For TM polarization mode, $n_{av} = 2.126$ and $p_h = 0.114$ μm. In the case of RG, the value is $n_{av} = 1.79$ and $p_h = 0.154$ μm in the TE polarization mode. For TM polarization mode, $n_{av} = 1.7$ and $p_h = 0.161$ μm. Similarly in the case of CC, $n_{av} = 1.75$ and $p_h = 0.139$ μm in the TE polarization and on the other hand $n_{av} = 1.78$ and $p_h = 0.136$ μm for the TM mode of polarization in CC beetle. The nanomechanical properties such as hardness and elastic modulus of RG beetle elytra were observed higher as compared to the Chrysidinae and CC. Its nanomechanical properties show that lesser depth of capacity is useful for designing the lightweight and high strength materials.

The observed reflectance spectra from the beetle elytra surface are significant due to disclosing the secrets of structural coloration based on nanostructures. They offer insights into the underlying nanostructural features, inspire biomimetic applications, and contribute to understanding the ecology and evolution in the natural world.

This article may be helpful to learn about the fabrication and design of photonic devices. Beetle elytra have also been selected as the biological prototype for the investigation to obtain the bio-inspirations for the design and development of light and strong materials.

## Acknowledgement

The authors thank the IIT Ropar for providing necessary facilities and infrastructure used in the present research. One of the author thanks SERB-DST for the NPDF fellowship (PDF/2017/01611).

## Funding Support

This work is supported by SERB-DST under the NPDF fellowship (PDF/2017/01611).

## Ethical Statement

This study does not contain any studies with human or animal subjects performed by any of the authors.

## Conflicts of Interest

The authors declare that they have no conflicts of interest to this work.

## Data Availability Statement

Data sharing is not applicable to this article as no new data were created or analyzed in this study.

## References


Berthier, S. (2007). *Iridescences: The physical color of insects.* USA: Springer. https://doi.org/10.1007/978-0-387-34120-0_1

Berthier, S., Boulenguez, J., & Bálint, Z. (2007). Multiscaled polarization effects in Suneve coronata (Lepidoptera) and other insects: Application to anti-counterfeiting of banknotes. *Applied Physics A*, *86*(1), 123–130. https://doi.org/10.1007/s00339-006-3723-9

Brink, D. J., van der Berg, N. G., Prinsloo, L. C., & Hodgkinson, I. J. (2007). Unusual coloration in scarabaeid beetles. *Journal of Physics D: Applied Physics*, *40*(7), 2189. https://doi.org/10.1088/0022-3727/40/7/050

Chen, J. X., Ni, Q. Q., Endo, Y., & Iwamoto, M. (2002). Distribution of trabeculae and elytral surface structures of the horned beetle, allomyrina dichotoma (linné) (coleoptera: Scarabaeidae). *Insect Science*, *9*(1), 55–61. https://doi.org/10.1111/j.1744-7917.2002.tb00143.x

Chen, J., Hao, N., Song, Y., Yang, J., & He, C. (2022). Shear properties of 3D-printed grid beetle elytron plates. *Journal of Materials Science*, *57*(35), 16974–16987. https://doi.org/10.1007/s10853-022-07659-x

Chen, J., & Wu, G. (2013). Beetle forewings: Epitome of the optimal design for lightweight composite materials. *Carbohydrate Polymers*, *91*(2), 659–665. https://doi.org/10.1016/j.carbpol.2012.08.061

Ching, S. Y., Li, G., Tam, H. L., Goh, D. T., Goh, J. K., & Cheah, K. W. (2014). Chirality in rhomborhina gigantea beetle. *Optical Materials Express*, *4*(11), 2340–2345. https://doi.org/10.1364/OME.4.002340

Clark-Hachtel, C. M., Linz, D. M., & Tomoyasu, Y. (2013). Insights into insect wing origin provided by functional analysis of vestigial in the red flour beetle, Tribolium castaneum. *Proceedings of the National Academy of Sciences*, *110*(42), 16951–16956. https://doi.org/10.1073/pnas.1304332110

Dehmel, R., Baumberg, J. J., Steiner, U., & Wilts, B. D. (2017). Spectrally resolved surface plasmon resonance dispersion using half-ball optics. *Applied Physics Letters*, *111*(20), 201102. https://doi.org/10.1063/1.4999636

England, G. T., Russell, C., Shirman, E., Kay, T., Vogel, N., & Aizenberg, J. (2017). The optical Janus effect: Asymmetric structural color reflection materials. *Advanced Materials*, *29*(29), 1606876. https://doi.org/10.1002/adma.201606876

Frantsevich, L., Dai, Z., Wang, W. Y., & Zhang, Y. (2005). Geometry of elytra opening and closing in some beetles (Coleoptera, Polyphaga). *Journal of Experimental Biology*, *208*(16), 3145–3158. https://doi.org/10.1242/jeb.01753

Fu, J., Yoon, B. J., Park, J. O., & Srinivasarao, M. (2017). Imaging optical scattering of butterfly wing scales with a microscope. *Interface Focus*, *7*(4), 20170016. https://doi.org/10.1098/rsfs.2017.0016

Gan, Z., Turner, M. D., & Gu, M. (2016). Biomimetic gyroid nanostructures exceeding their natural origins. *Science Advances*, *2*(5), e1600084. https://doi.org/10.1126/sciadv.1600084

Gorb, S. N., Beutel, R. G., Gorb, E. V., Jiao, Y., Kastner, V., Niederegger, S., …, & Vötsch, W. (2002). Structural design and biomechanics of friction-based releasable attachment devices in insects. *Integrative & Comparative Biology*, *42*(6), 1127–1139. https://doi.org/10.1093/icb/42.6.1127

Gorb, S. N., & Goodwyn, P. P. (2003). Wing-locking mechanisms in aquatic Heteroptera. *Journal of Morphology*, *257*(2), 127–146. https://doi.org/10.1002/jmor.10070

Grier, D. G. (2003). A revolution in optical manipulation. *Nature*, *424*(6950), 810–816. https://doi.org/10.1038/nature01935

Guo, C., Li, D., Lu, Z., Zhu, C., & Dai, Z. (2014). Mechanical properties of a novel, lightweight structure inspired by beetle's elytra. *Chinese Science Bulletin*, *59*(26), 3341–3347. https://doi.org/10.1007/s11434-014-0384-5

Guo, C., Song, W., & Dai, Z. (2012). Structural design inspired by beetle elytra and its mechanical properties. *Chinese Science Bulletin*, *57*(8), 941–947. https://doi.org/10.1007/s11434-011-4956-3

Heepe, L., Wolff, J. O., & Gorb, S. N. (2016). Influence of ambient humidity on the attachment ability of ladybird beetles (Coccinella septempunctata). *Beilstein Journal of Nanotechnology*, *7*, 1322–1329. https://doi.org/10.3762/bjnano.7.123

Iwamoto, M., Chen, J., Kurashiki, K., & Ni, Q.-Q. (2002). Chitin fibre and its laminated structure of the fore-wing of beetle. *WIT Transactions on the Built Environment*, 59, 127–136.

Karthaus, O. (2012). *Biomimetics in photonics*. USA: CRC Press.

Kertész, K., Baji, Z., Deák, A., Piszter, G., Rázga, Z., Bálint, Z., & Biró, L. P. (2021). Additive and subtractive modification of butterfly wing structural colors. *Colloid and Interface Science Communications*, *40*, 100346. https://doi.org/10.1016/j.colcom.2020.100346

Kinoshita, S. (2008). *Structural colors in the realm of nature*. Singapore: World Scientific.

Koch, K., Bhushan, B., & Barthlott, W. (2009). Multifunctional surface structures of plants: An inspiration for biomimetics. *Progress in Materials Science*, *54*(2), 137–178. https://doi.org/10.1016/j.pmatsci.2008.07.003

Lam, L., Chen, W., Hao, H., Li, Z., & San Ha, N. (2023). Dynamic crushing performance of bio-inspired sandwich structures with beetle forewing cores. *International Journal of Impact Engineering*, *173*, 104456. https://doi.org/10.1016/j.ijimpeng.2022.104456

Lee, N., Berthelson, P. R., Nguyen, V., Garrett, M. L., Brinda, A. K., Moser, R. D., …, & Prabhu, R. K. (2021). Microstructure and nanomechanical properties of the exoskeleton of an ironclad beetle (Zopherus haldemani). *Bioinspiration & Biomimetics*, *16*(3), 036005. https://doi.org/10.1088/1748-3190/abe27b

Li, L., Guo, C., Li, X., Xu, S., & Han, C. (2017). Microstructure and mechanical properties of rostrum in Cyrtotrachelus longimanus (Coleoptera: Curculionidae). *Animal Cells and Systems*, *21*(3), 199–206. https://doi.org/10.1080/19768354.2017.1330764

Linz, D. M., Hu, A. W., Sitvarin, M. I., & Tomoyasu, Y. (2016). Functional value of elytra under various stresses in the red flour beetle, Tribolium castaneum. *Scientific Reports*, *6*(1), 34813. https://doi.org/10.1038/srep34813

Liu, F., Yin, H., Dong, B., Qing, Y., Zhao, L., Meyer, S., …, & Chen, B. (2008). Inconspicuous structural coloration in the elytra of beetles Chlorophila obscuripennis (Coleoptera). *Physical Review E*, *77*(1), 012901. https://doi.org/10.1103/PhysRevE.77.012901

Lloyd, V. J., & Nadeau, N. J. (2021). The evolution of structural colour in butterflies. *Current Opinion in Genetics & Development*, *69*, 28–34. https://doi.org/10.1016/j.gde.2021.01.004

Michelson, A. A. (1911). LXI. On metallic colouring in birds and insects. *The London, Edinburgh, and Dublin Philosophical Magazine and Journal of Science*, *21*(124), 554–567. https://doi.org/10.1080/14786440408637061

Mouchet, S. R., Verstraete, C., Bokic, B., Mara, D., Dellieu, L., Orr, A. G., …, & Kolaric, B. (2023). Revealing natural fluorescence in transparent insect wings by linear and

nonlinear optical techniques. *Journal of Luminescence*, *254*, 119490. https://doi.org/10.1016/j.jlumin.2022.119490

Neville, A. C., & Caveney, S. (1969). Scarabaeid beetle exocuticle as an optical analogue of cholesteric liquid crystals. *Biological Reviews*, *44*(4), 531–562. https://doi.org/10.1111/j.1469-185X.1969.tb00611.x

Oliver, W. C., & Pharr, G. M. (2004). Measurement of hardness and elastic modulus by instrumented indentation: Advances in understanding and refinements to methodology. *Journal of Materials Research*, *19*(1), 3–20. https://doi.org/10.1557/jmr.2004.19.1.3

Ospina-Rozo, L., Priscilla, N., Hutchison, J. A., van de Meene, A., Roberts, N. W., Stuart-Fox, D., & Roberts, A. (2023). Deconstructed beetles: Bilayered composite materials produce green coloration with remarkably high near-infrared reflectance. *Materials Today Advances*, *18*, 100363. https://doi.org/10.1016/j.mtadv.2023.100363

Parker, A. R. (2000). 515 million years of structural colour. *Journal of Optics A: Pure and Applied Optics*, *2*(6), R15. https://doi.org/10.1088/1464-4258/2/6/201

Reddi, S., Jain, A. K., Yun, H. B., & Reddi, L. N. (2012). Biomimetics of stabilized earth construction: Challenges and opportunities. *Energy and Buildings*, *55*, 452–458. https://doi.org/10.1016/j.enbuild.2012.09.024

Scharf, T. (2007). *Polarized light in liquid crystals and polymers*. USA: Wiley.

Sharma, V., Crne, M., Park, J. O., & Srinivasarao, M. (2009). Structural origin of circularly polarized iridescence in jeweled beetles. *Science*, *325*(5939), 449–451. https://doi.org/10.1126/science.1172051

Srinivasarao, M. (1999). Nano-optics in the biological world: Beetles, butterflies, birds, and moths. *Chemical Reviews*, *99*(7), 1935–1962. https://doi.org/10.1021/cr970080y

Starkey, T., & Vukusic, P. (2013). Light manipulation principles in biological photonic systems. *Nanophotonics*, *2*(4), 289–307. https://doi.org/10.1515/nanoph-2013-0015

Sun, J., Wu, W., Song, Z., Tong, J., & Zhang, S. (2019). Bio-inspirations for the development of light materials based on the nanomechanical properties and microstructures of beetle Dynastes tityus. *Journal of Bionic Engineering*, *16*(1), 154–163. https://doi.org/10.1007/s42235-019-0014-7

Vigneron, J. P., Pasteels, J. M., Windsor, D. M., Vértesy, Z., Rassart, M., Seldrum, T., . . . , & Welch, V. (2007). Switchable reflector in the Panamanian tortoise beetle Charidotella egregia (Chrysomelidae: Cassidinae). *Physical Review E*, *76*(3), 031907. https://doi.org/10.1103/PhysRevE.76.031907

Wang, S., McNamara, M. E., Wang, B., Hui, H., & Jiang, B. (2023). The origins of colour patterns in fossil insects revealed by maturation experiments. *Proceedings of the Royal Society B*, *290*(2007), 20231333. https://doi.org/10.1098/rspb.2023.1333

Wu, W., Wang, Y., & Sun, J. (2023). The mechanical implementations in three kinds of color-changing beetle elytra. *Bioinspired, Biomimetic and Nanobiomaterials*, *12*(1), 29–38. https://doi.org/10.1680/jbibn.22.00074

Yu, M., Hermann, I., Dai, Z., & Gitis, N. (2013). Mechanical and frictional properties of the elytra of five species of beetles. *Journal of Bionic Engineering*, *10*(1), 77–83. https://doi.org/10.1016/S1672-6529(13)60201-2

Zhang, Q., Yu, H., Barbiero, M., Wang, B., & Gu, M. (2019). Artificial neural networks enabled by nanophotonics. *Light: Science & Applications*, *8*(1), 42. https://doi.org/10.1038/s41377-019-0151-0

Zhao, Y., Xie, Z., Gu, H., Zhu, C., & Gu, Z. (2012). Bio-inspired variable structural color materials. *Chemical Society Reviews*, *41*(8), 3297–3317. https://doi.org/10.1039/C2CS15267C

Zhou, L., He, J., Li, W., He, P., Ye, Q., Fu, B., . . . , & Shang, W. (2019). Butterfly wing hears sound: Acoustic detection using biophotonic nanostructure. *Nano Letters*, *19*(4), 2627–2633. https://doi.org/10.1021/acs.nanolett.9b00468

Zhou, M., Huang, D., Su, X., Zhong, J., Hassanein, M. F., & An, L. (2020). Analysis of microstructure characteristics and mechanical properties of beetle forewings, Allomyrina dichotoma. *Materials Science and Engineering: C*, *107*, 110317. https://doi.org/10.1016/j.msec.2019.110317

Zhou, M., Xie, J., Chen, J., Liu, C., & Tuo, W. (2015). The influence of processing holes on the flexural properties of biomimetic integrated honeycomb plates. *Materials & Design*, *86*, 404–410. https://doi.org/10.1016/j.matdes.2015.07.060

**How to Cite:** Jyoti, J., & Tripathy, S. (2024). Role of Micro-Architectures on Insects' Elytra Affects the Nanomechanical and Optical Properties: Inspired for Designing the Lightweight Materials. *Journal of Optics and Photonics Research*. *1*(1), 32–42. https://doi.org/10.47852/bonviewJOPR32021587